

Galaxies Beyond the Milky Way

AA2052

Available as a module for a *University Advanced Certificate*,
CertHE, *DipHE* and *BSc in Astronomy*.

Sample Notes

These sample pages from the Course Notes for the module *Galaxies Beyond the Milky Way* have been selected to give an indication of the level and approach of the course. They are not designed to be read as a whole, but are intended to give you a flavour of the syllabus, style, diagrams, images, equations, mathematical content and presentation. They are a subset of the colour, navigable on-line version of the learning materials.

All enrolled students have access to the Course Materials via the course website.

- All sections of notes will be available in modest colour and basic navigation in pdf format suitable for downloading and printing at home.
- The learning materials consist of 6 sections of notes, some of which include short case studies.
- The module assumes prior study of *AA2051 The Milky Way*.

July 2008

The Local Universe






Observations over a broad range of wavelengths reveal the structure and components of nearby galaxies in great detail. These observations together with theoretical models and numerical simulations lead us to a deeper understanding of how such structures form and evolve dynamically. We begin this module AA2052 (Galaxies beyond the Milky Way) with a study of the appearance and content of nearby galaxies – those within about 40 Mpc of us, i.e. at redshifts $z < 0.01$, with look-back times of only a very small fraction of the age of the universe.

When a telescope is used to look out at the universe it reveals many extended objects. Some of these such as planetary nebulae and supernova remnants are within our own Galaxy but most are much further away. They are the galaxies, which are made up of stars, interstellar gas and dust, all of which we can detect, and also dark matter, the presence of which we can infer from movements of material within the galaxies. There are no sharp edges to galaxies: they can look different in images of different exposure levels. In AA2051 *The Milky Way*, we learnt about our Galaxy. Other galaxies can be very different. In this module AA2052 *Galaxies Beyond the Milky Way*, we will explore the properties of other galaxies, contrasting them with our own Galaxy, and investigating when and how they were made and how they have changed over time.

This first Section concentrates on the observational properties of galaxies in the nearby universe. By “nearby” we mean that the distances involved correspond to look-back times of only a very small fraction of the age of the universe. On the scales of the nearby universe, galaxies have not evolved much with time. (Recall that when we observe galaxies at larger distances we are looking back further in time because of the finite speed of light). This section contains several images of different galaxy types, but there are many more examples available to view on the web: these illustrate the magnificence and beauty of galaxy structures.

The **morphology** of a galaxy means its physical appearance in an image. The use of this appearance to classify galaxies is described below.

ICON KEY

	Valuable information
	Test yourself
	Worked example
	Textbook
	Important Equation

Galaxies

described in *AA1051*) then allows us to model the evolution of these populations, and hence to predict observables such as colours, magnitudes and spectral features as a function of time. Realistic models also account for mass loss from stars during their lifetimes, as well as changes in metal content with time. Two quantities that control the numbers and ages of stars in a galaxy are the initial mass function and the star formation rate. These quantities and their parameterisation in models are explained below.

Initial Mass Function (IMF)

In a population of stars, the distribution of numbers of stars with different masses, made when the population *first* formed, is known as the **initial mass function**. From observations of young star clusters in our Galaxy we know that there are many more low mass stars formed than high mass stars. **Salpeter** showed from such observations that this distribution is approximately a power law, over a large range of stellar masses. This can be written as:-

Salpeter IMF



$$\xi(M) = AM^{-(\beta+1)} \tag{Equation 1.4}$$

where $\xi(M)dM$ is the number fraction of stars in the mass interval dM , around mass M ; β is a constant (normally approximately 1.35, giving an overall index of -2.35 as in the **Salpeter IMF**, *AA2051 Notes* Equation 2.5). In Section 2 of *AA2051 Milky Way Notes* we used the IMF in absolute units, *i.e.* numbers of stars born per pc^3 ($A = 1$) but it is more convenient here to normalise the IMF. Hence, here A is a normalisation constant, obtained by requiring the total mass fraction of stars to be equal to 1, *i.e.*:-

Normalisation



$$\int_{m_L}^{m_U} M \xi(M) dM = 1 \tag{Equation 1.5}$$

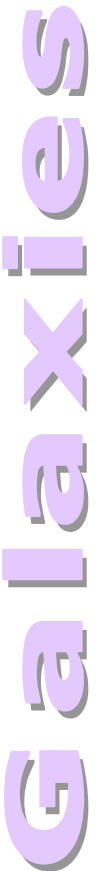
This means that the sum (or integral) of the fractional mass contribution of stars of all different masses is unity in the mass range m_L to m_U . In practice these limits are $m_L \approx 0.1M_{\odot}$ (the numbers of stars with smaller masses are uncertain but they contribute little to the overall mass of stars) and $m_U \approx 100M_{\odot}$. There are very few stars with higher mass, so any above this limit will also contribute little to the overall mass of stars.

Worked Example

As an example, we find the mass fraction of stars with masses less than the sun ($1.0 M_{\odot}$). This is equal to the integral of $[M\xi(M)dM]$ between m_L and M_{\odot} . Substituting for $\xi(M)$ from Equation 1.4,

$$A \int_{m_L}^{M_{\odot}} M^{-\beta} dM = A \left[\frac{M^{-\beta+1}}{1-\beta} \right]_{m_L}^{M_{\odot}} = \frac{A}{(1-\beta)} [M_{\odot}^{-\beta+1} - m_L^{-\beta+1}]$$

We do not need to know A since we can divide by the normalisation equation (mass for all stars).



$$A \int_{m_L}^{m_U} M^{-\beta} dM = 1 \quad (\text{from Equation 1.5})$$

Thus the mass fraction in stars $< 1.0 M_{\odot}$ is:
$$\frac{[M_{\odot}^{1-\beta} - m_L^{1-\beta}]}{[m_U^{1-\beta} - m_L^{1-\beta}]}$$

And for $\beta = 1.35$, this gives the mass fraction = 0.607.

Here we have adopted the same approach as in *AA2051* Box 4.1, but have slightly generalised the formula by leaving the index as a parameter (to allow for steeper or shallower IMFs) and leaving the upper and lower mass limits as symbols rather than substituting specific values for these.

Exercise 5



For a Salpeter IMF ($\beta=1.35$), what is the mass fraction of stars with:

- i) mass $M > 1.0 M_{\odot}$
- ii) mass $M > 10 M_{\odot}$ and where will most of this mass end up after a single generation of stars?

It is difficult to determine the IMF from observed mass functions (of older stars). However, observations of different populations of stars in our Galaxy indicate *little variation* of the IMF from place to place. This is an important result since it implies that the fragmentation of gas clouds and formation of stars from condensed gas operates in the same way across the Galaxy. We expect to observe some differences in the IMF for very different conditions; in particular, primordial gas from the big bang contains essentially no metals, which act to cool the gas more efficiently. So we expect the collapse of primordial gas clouds to take longer, leading to a different (possibly top heavy) IMF. Quantifying variations amongst IMFs in different environments will be one of the challenges for the Next Generation (James Webb) Space Telescope (JWST).

Star Formation Rate (SFR)

The star formation rate describes the mass of stars formed per unit time. This will depend on many things, for example:

- **Gas density.**
- **Heating and cooling processes** in the ISM will determine if gas can collapse to high enough densities for star formation to proceed.
- The **metallicity** of the ISM affects the cooling rate. Enrichment and mixing of stellar ejecta affect the metallicity for subsequent generations of stars.
- **Mass loss** from stars may dissociate and blow away the molecular cloud from which those stars were formed, thus limiting further star formation, or collisions of gas clouds may lead to further random star formation.
- **Magnetic fields** affect gas motions and the magnetic energy helps resist cloud collapse (*cf.* Section 3 of *Milky Way Notes*).

- **High-energy particles** (cosmic rays) can penetrate molecular clouds and dissociate molecules.

In practice it is difficult to measure the effect of these processes on SFRs. The first factor, gas density, is usually assumed to dominate. Observations (Figure 1.10) show that higher gas densities generally lead to higher rates of star formation. Therefore the SFR is often described by a power law dependence on gas mass density (ρ):-

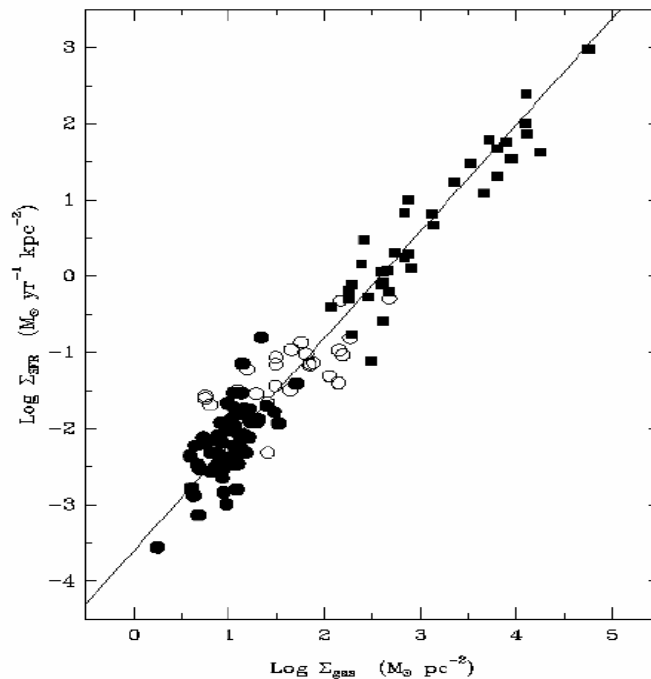
Schmidt Law



$$SFR = \frac{dS}{dt} = A\rho^n \tag{Equation 1.6}$$

This is the **Schmidt law**, named after the person who showed it to be approximately true. Here S is the total star mass per unit volume, A is a normalisation constant and n is the index (often taken to be about 1). Figure 1.10 shows observational evidence in support of the Schmidt law, in a sample of disc galaxies.

Figure 1.10
Observed trend of SFR (measured from $H\alpha$ observations) with gas density (atomic and molecular) in a sample of disc galaxies.
Image credit: Kennicutt 1998, ApJ, 498, 541.



Worked Example



For a gas cloud of mass $10^6 M_\odot$ per unit volume, how long will it take the gas mass to be halved, assuming an initial star formation rate of $10^6 M_\odot \text{ Gyr}^{-1}$ per unit volume?

Assume a Schmidt law for the SFR (with $n = 1$). The change in gas mass is equal and opposite to the change in star mass (ignoring stellar mass loss). Thus, in a unit volume:

$$SFR = A\rho = \frac{dS}{dt} = -\frac{d\rho}{dt} \tag{Equation 1.7}$$

Given the initial SFR, \mathcal{A} must be equal to 1.0 Gyr^{-1} . Re-arranging the above equation to gather terms involving the same variable together gives:

$$\frac{d\rho}{\rho} = -dt \quad (\text{with time in units of Gyr})$$

Then integrate this for when $\rho_0 = 10^6$ is the initial gas density and T is the time to be evaluated:

Remember : the integral of $1/\rho$ is $\ln(\rho)$.

$$\int_{\rho_0}^{\rho_0/2} \frac{d\rho}{\rho} = \int_0^T -dt$$

$$\Leftrightarrow T = [\ln \rho]_{\rho_0/2}^{\rho_0} = \ln \rho_0 - \ln \frac{\rho_0}{2}$$

$$= \ln 2 = 0.69$$

So time for half the gas to be used is: $T \equiv 0.69 \text{ Gyr}$.

Interstellar Medium

Within galaxies the space between stars is filled with gas in several temperature phases together with dust particles made of cold, heavy elements. Properties of the inter-stellar medium (ISM) differ across the Hubble types.

Spiral and Irregular galaxies.

Cold, neutral gas (at a few 10s of degrees Kelvin) is found in large quantities in late-type galaxies (S and Irr). In Section 6 of *A42051*, we saw how the **21-cm radio emission** of neutral hydrogen can be used to detect extended gas distributions and to map the spiral structure of our Milky Way. The emission line in question is due to the **spin-flip transition** of neutral hydrogen. The quantised spin of the orbital electron can be either parallel or anti-parallel to the spin of the nucleus, with a small difference in the corresponding energy levels. Although this transition has a very low probability of occurring (it is said to be **forbidden**) the large quantities of neutral hydrogen in the universe mean that the resultant 21cm line is a useful probe of cold gas in our own Galaxy and other galaxies. In many cases the cold gas extends beyond the starlight and allows the mass distribution at large radii to be measured.

The cold gas resides in clouds that are in **pressure equilibrium** with a more diffuse, hotter (10^4 K) interstellar gas, which is partially ionised. Even denser and more compact are the molecular clouds, which are potential sites of new star formation. A schematic illustration of the multi-phase nature of the ISM is shown in Figure 1.11. The central slightly flattened spheroid is the bulge; the more extended structure is the disc seen from the plane of the galaxy; dark blobs represent globular clusters extending into the roughly spherical halo of the galaxy. The ISM components are illustrated as dense molecular clouds in the disc embedded in more diffuse atomic and partially ionised clouds which in turn are surrounded by hotter, diffuse, ionised gas in the disc. The star on the left indicates

Galaxy Shapes and Support Mechanisms

In the discs of spiral galaxies the stellar kinematics are dominated by systematic rotational motion of a few hundred km s^{-1} plus smaller more random motions resulting in a velocity dispersions of a few tens of km s^{-1} . In spheroidal systems, such as elliptical galaxies, the bulges of spiral and lenticular galaxies, and globular clusters, random velocity dispersion is the more important. Figure 2.4 shows the relative importance of the observed maximum rotational velocity v_m compared with the average observed stellar velocity dispersion $\bar{\sigma}$ for different types of spheroids.

Figure 2.4 shows that normal (giant) ellipticals (open circles) tend to have very low rotational velocities, with few exceptions. Most of their kinetic energy, supporting the stellar system against further collapse, is in random velocity dispersion. The slightly flattened shapes of bright (giant) ellipticals are thus not supported by rotation. In fact they are supported by the velocity dispersion of their stars (analogous to pressure support in a gas) and anisotropy in their velocity dispersion gives them their slightly flattened shape. In contrast, Figure 2.4 also shows that points for low luminosity ellipticals and spiral bulges lie close to the line expected for rotationally supported, oblate stellar systems. They have significant kinetic energy in velocity dispersion but their rotation is enough to give them their slightly flattened shapes, without invoking other mechanisms.

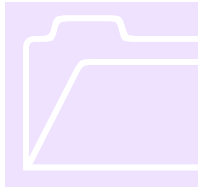
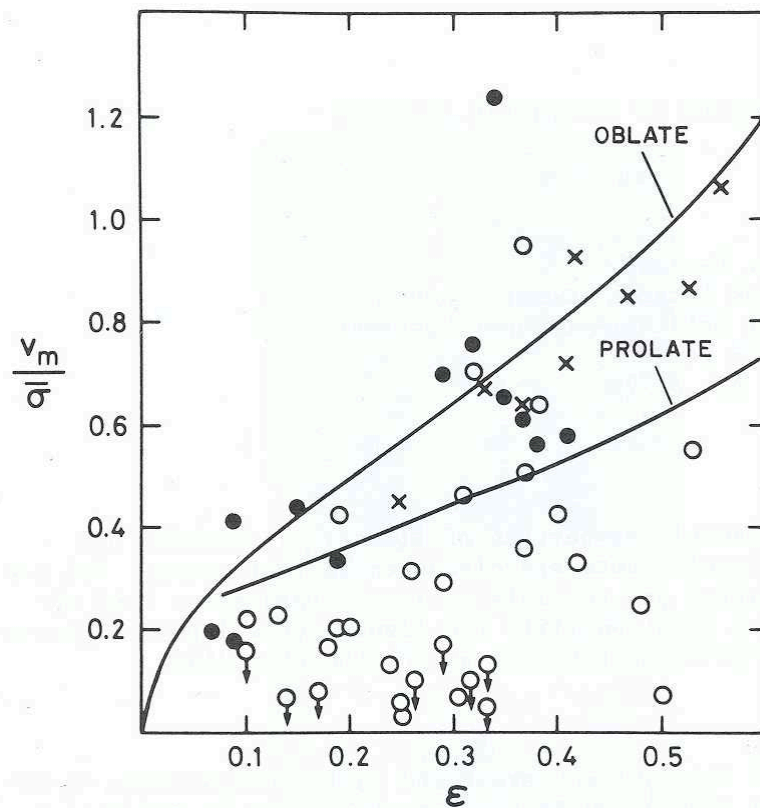


Figure 2.4 Maximum rotation velocity v_m divided by average velocity dispersion $\bar{\sigma}$ plotted against galaxy ellipticity ϵ for various types of spheroidal systems: open circles are giant ellipticals, filled circles are faint ellipticals and crosses are spiral bulges. The lines indicate model predictions for rotationally-supported oblate and prolate stellar systems.
Image credit: Davies 1987, IAU Symposium No. 127.



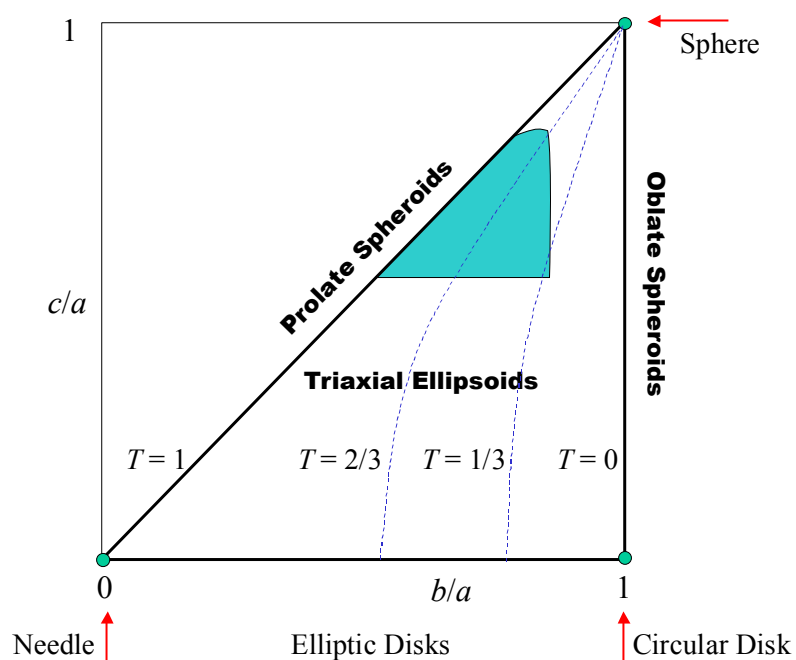
In the case of giant ellipticals, the dispersion must be different in different directions (i.e. **anisotropic**) for it to support a flattened structure. These galaxies,

whose shape is determined by non-isotropic σ , can be **oblate**, like a slightly flattened orange, **prolate**, like a rugby ball, or **triaxial**, with all three principal axes differing in scale length. Figure 2.5 illustrates the range of parameter space covered by the scale-lengths of these intrinsic axes, where a is the longest axis length, b is the intermediate axis length and c is the shortest axis length. The **triaxiality parameter** is defined by:

$$T = \frac{1 - (b/a)^2}{1 - (c/a)^2} \tag{EQUATION 2.3}$$

Thus $T = 0$ for oblate spheroids, $T = 1$ for prolate spheroids and takes intermediate values for triaxial ellipsoids.

Figure 2.5 “Ellipsoid land” (adapted from a plot by de Zeeuw and Franx, 1991, Ann Rev A&A, Vol. 29, p239, their fig.1). The shaded area represents the allowed range for NGC 4261 (see the case study below).



Exercise 1

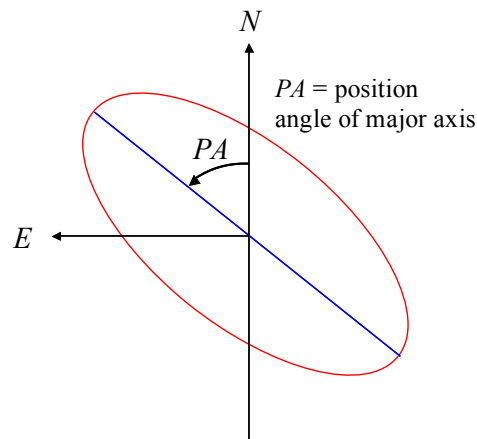


For a triaxial ellipsoid whose true (shortest/longest) axis ratio is $c/a = 0.5$, with $T = 0.34$, what is the value of b/a ?

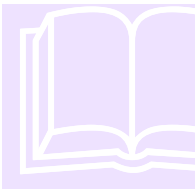
Position Angle

The orientation of an astronomical object on the celestial sphere is conveniently specified by the **position angle** and is the angle (in degrees) measured in the plane of the sky from north in an eastward direction. Figure 2.6 illustrates the position angle of the apparent major axis of an elliptical galaxy.

Figure 2.6 Diagram to show definition of position angle of apparent major axis of a galaxy, measured in an easterly direction from north. Remember that on the celestial sphere East lies to the left of North.



CASE STUDY



NGC 4261 , A Prolate Elliptical

(References: Davies and Birkinshaw, 1986, *ApJ*, **303**, L45; Jaffe *et al*, 1993, *Nature*, **364**, 213; Jaffe *et al*, 1996, *ApJ*, **460**, 214.)

From photometric images of the E2 elliptical galaxy NGC 4261, the apparent major axis (longer axis observed on the sky) lies at the same position angle (E of N) $159^\circ \pm 2^\circ$, for all regions of the galaxy from the central 2 arcseconds radius region to regions as much as 150 arcseconds from the galaxy's centre. Therefore the apparent minor axis is 90° away from this at 69° (see Figure 2.7). The ellipticity ($1 - b/a \sim 0.17$) also does not vary much over this measured range. There are no strong dust lanes to distort the photometric measurements. Therefore this is a fairly regular elliptical galaxy with no twisting of the isophotes. There are some constraints on the galaxy's intrinsic three-dimensional shape imposed by the observed two-dimensional shape. We know the galaxy cannot be highly spherical since projected ellipticity is generally smaller (rounder) than the intrinsic ellipticity of a spheroid, and the observations show that NGC 4261 is not a round galaxy in projection onto the celestial sphere.

NGC 4261 was observed with long-slit spectroscopy to determine its kinematic properties, with the slit at four orientations. The surprising result was that the greatest amplitude of rotation occurs along a line at position angle 71° , approximately *along* the apparent **minor axis**. Such **minor axis rotation** (= rotation *about* the apparent *major* axis) is indicative of a prolate spheroid. Modelling of the observed kinematics suggests that a projection of the true rotation axis, onto the plane of the sky, lies at $153^\circ \pm 4^\circ$, which is within $6^\circ \pm 4^\circ$ of the apparent major axis. For such a system to be stable, the axis of rotation is likely to lie along the true major axis like a spindle. Another, less likely configuration is a tumbling prolate spheroid, in the way that a bar appears to move in a spiral galaxy. For NGC 4261 this second configuration is less likely since it would only fit the data for a rather restricted range of possible viewing angles, whereas the first possibility (like a spindle) is true for almost all possible viewing angles. Can you think of an orientation relative to the line of sight to the observer for which this is not so? *I.e.* when would the axis of rotation *not* appear to lie along the apparent major axis of a prolate galaxy spinning about its major axis?






S E I X I A I G

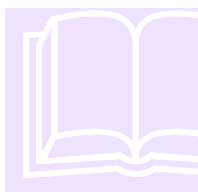
The Local Group

Most galaxies lie in groups and our Milky Way Galaxy is no exception. It lies in a small group of galaxies that move together through the universe, attracted by superclusters distributed on larger scales.

The Milky Way Galaxy is a member of a small clan of a few tens of galaxies, mostly dwarfs, known as the **Local Group**. This group is a gravitationally bound system that will evolve with time through galaxy interactions under the influence of gravity. The importance of these nearest galaxies for astronomers is that galaxy properties can be studied in great detail. Knowledge gained from these nearby galaxies can then be applied to better understand more distant galaxies and groups. Individual stars are resolved in the nearest galaxies, so stellar populations can be studied through the Hertzsprung-Russell diagram to uncover the stellar composition, distances and ages, and to provide an insight into stellar kinematics and dynamics. Unusual chemical compositions provide evidence of past destruction of **satellite** galaxies by the **giant spiral galaxies**, the Milky Way and Andromeda (M31). The future of the Local Group has been simulated numerically, revealing how our local region of the universe will change over the next few billion years. In this Section we will explore these aspects of our nearest galaxies.

ICON KEY

	Valuable information
	Test yourself
	Worked example
	Textbook
	Important Equation



In conjunction with this Section of Notes, you should read the whole of Chapter 4 of *SG*, excluding 4.1.4.

Morphology and Distribution

Overview

The Local Group is an irregular structure of about 40 known galaxies, mostly dIrr and dSph types. These are largely clustered around two giant spirals: the Milky Way (an Sbc) and the slightly larger Andromeda galaxy (M31, an Sb) about 730 kpc apart. A third, moderate sized spiral (M33, an Sc) lies quite close to the M31 subgroup. Figure 3.1 illustrates the distribution of different galaxy types in the Local Group. For a movie which pans around an illustration of the Local Group see http://www.star.uclan.ac.uk/~aes/LG_movie.mpeg. More dwarf galaxy members of the Local Group continue to be discovered: recent additions are Cetus, Antlia and Sagittarius, (see *e.g. Universe*, Figure 26 -19). There are unlikely to be any

luminous, giant galaxies yet to be discovered in the Local Group since these are the easiest types to find. They stand out as resolved objects against the night sky and would have been detected in various sky surveys. The low surface brightness galaxies, mentioned in Section 1, and fainter dwarf galaxies are probably some of the most difficult to find. Therefore there may be more of these yet to be discovered in the Local Group. Additional members of the Local Group may also be lurking behind the bright plane of the Milky Way where it is more difficult to detect galaxies.

Figure 3.1
Illustration of the distribution of galaxies in the Local Group, showing galaxies colour-coded according to their type.
Image credit: Brandner and Grebel 1998.

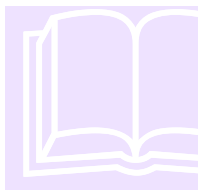
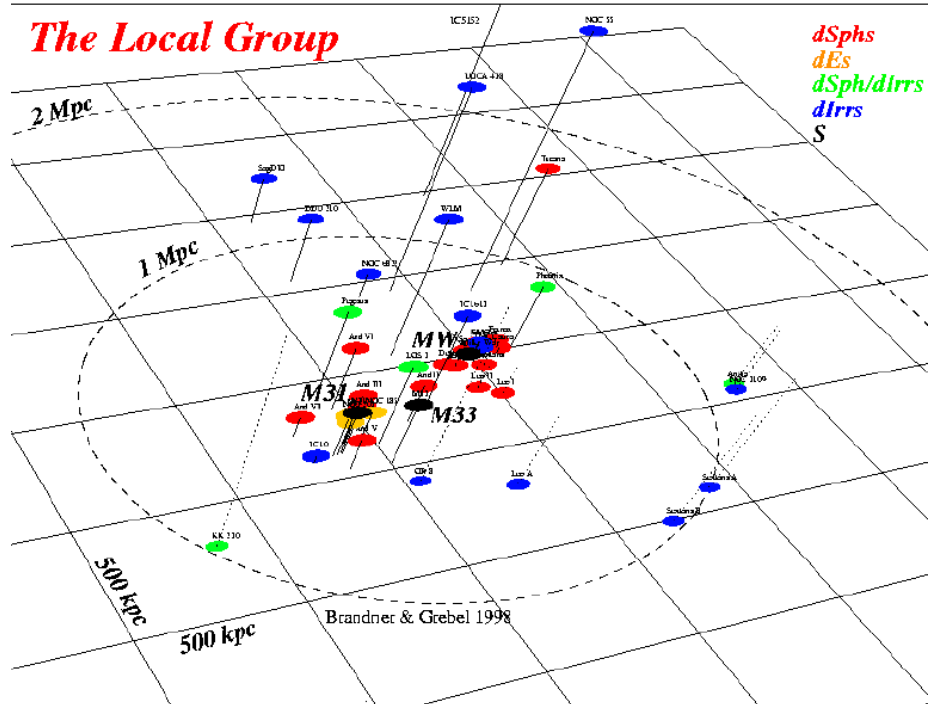


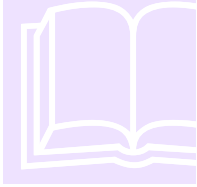
Table 3.1 summarises the currently known members of the Local Group, in order of increasing distance from our Galaxy. This table was compiled from tables in *Sparke & Gallagher*, table 4.1; and *Binney & Merrifield*, table 4.3. See these tables for an alternative ordering, in terms of luminosity. Also, *The Galaxies of the Local Group*, by *S. van den Bergh*, table 2.1 lists the galaxies by Right Ascension. From Table 3.1 we see that the Local Group is about 1 Mpc in radius, with **two sub-groups** centred around the two giant spirals, the Milky Way and Andromeda, plus a few more widely distributed galaxies, mostly dwarfs (dSph *e.g.* Figure 1.4 right, dIrr and dE).

For some of the more distant galaxies, group membership has still to be confirmed. There is no sharp edge to the Local Group and there are other groups not far beyond it. For example, there is a group around the Sb galaxy M81 at a distance of about 3.7 Mpc from the Milky Way, and other groups lie even closer. Therefore assignment of outlying galaxies to a particular group becomes somewhat ambiguous. One selection criterion typically used is that galaxies within a distance of 1.5 Mpc are candidates for Local Group membership.

Galaxies

poor populations and can be identified from their variability-luminosity-colour properties.

CASE STUDY 1

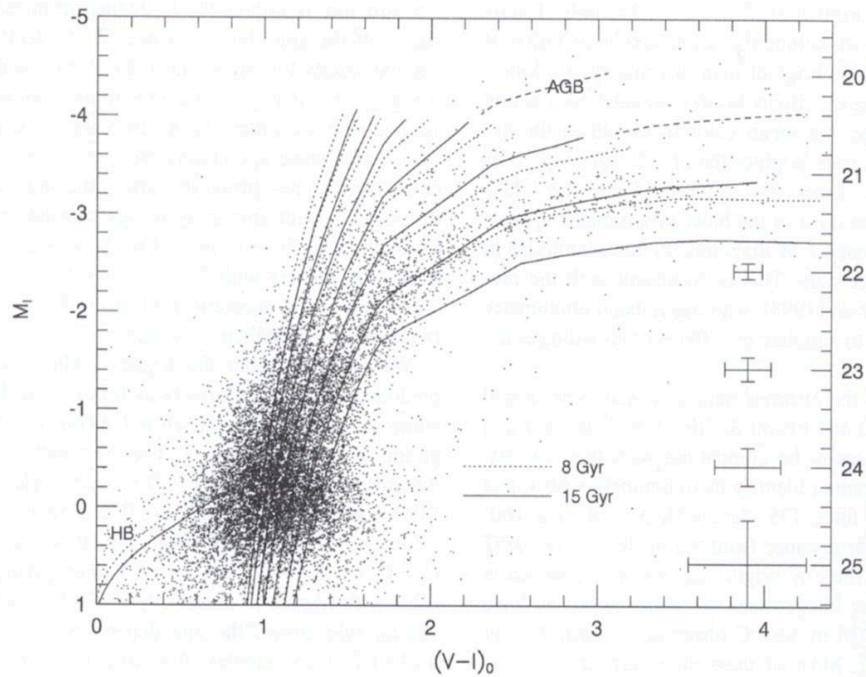


M32 - A metal rich, compact elliptical, with a wide range of metallicities.

(References: *Grillmair et al*, 1996, AJ, 112, 1975; *Mateo* 1998, *Ann. Rev. A&S*, Vol 36; *Van den Bergh*, 2000, chapter 8).

In this study, using photometric observations obtained from images taken with HST, the RGB was used to constrain the metal properties of the stellar population in M32. Figure 3.7 shows the data for about 20000 stars, plotted as dots in a C-M diagram. The vertical axis is absolute magnitude in the near-infrared I band (M_I) and the horizontal axis is the visual minus I band colour corrected for interstellar reddening along the observer's line-of-sight ($(V-I)_0$). The apparent I magnitude is indicated on the right of the plot. Model **isochrones** (locations of stars of different masses, with the same age) are shown for RGB, AGB and HB stars. The RGB models range in metallicity from 1/16th solar to solar, from left to right. The younger (dotted) lines show the small effect that age differences have on the RGB isochrones. Two intermediate metallicity isochrones for the asymptotic giant branch, extending redward of the RGBs are shown. There are very few AGB stars in M32. The theoretical location of the HB is shown for two ages. There is no evidence of a HB in M32, only a massive red clump at the red end of the HB. These RC stars are an indicator of the presence of **intermediate age stars** (several Gyr old), since a RC is seen in Galactic globular clusters of intermediate age.

Figure 3.7 C-M diagram for M32 from HST observations. Theoretical isochrones for 7 different metallicities and two ages are superimposed on the RGB. Typical error bars for the observations are shown on the right, within the plot. The right-hand scale is apparent magnitude in the I band (m_I).
Image credit: Grillmair et al, 1996, AJ, 112, 1975



The RGB isochrones in Figure 3.7 show that M32 has stars with a **wide range of metallicities**: the observed RGB is very broad, over and above measurement errors. From the brighter stars, with smaller errors, the relative numbers of stars

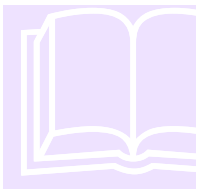
with different metallicities were found. These ranged from 0.03 to 1.25 times solar metallicity, with a peak at about 0.6 times the metallicity of the Sun.

Such resolved star observations are more reliable when taken *above* the Earth's atmosphere. For example, ground-based, resolved-star observations of M32 suggested that there was a luminous, red AGB population, implying the presence of a younger stellar population of a few Gyr. With better spatially resolved data from space observations, this was shown to be a spurious result of image crowding: two blurred star images can look like one, intrinsically brighter star on a CCD image – thus leading to a spurious population of luminous stars.

A complementary approach to the C-M diagram analysis is to obtain integrated spectra of a population. In principle, individual spectral features can tell us about the age and metallicity of a stellar population. However, in practice this is fraught with difficulties and degeneracies between age and metallicity effects. Nevertheless, integrated spectra are the only option for more distant, and therefore unresolved, stellar populations. M32 can be studied in both ways because it is bright enough and near enough for both resolved star observations (C-M diagrams) and integrated light observations (spectra) to be possible. Therefore M32 will provide a useful link between these two methods as they become more fully developed.

In summary, the C-M diagram of M32 reveals old/intermediate age stars with a well defined, wide range of metallicities. Would other elliptical galaxies all look similar if we could resolve them?

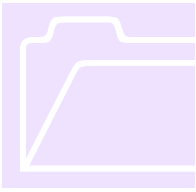
CASE STUDY 2



Phoenix dwarf – A composite population of young and old stars.

(References: *Holtzman, Smith & Grillmair*, 2000, *AJ*, 120, 3060; *Mateo* 1998, *Ann. Rev. Astr. & A.*, Vol 36).

HST observations were again used to obtain a C-M diagram for the Phoenix dwarf galaxy: Figure 3.8 plots apparent magnitude in the I band versus V-I colour. Error bars on the right indicate observational errors at different apparent magnitudes (I). Each point represents a star and there are many thousands of stars plotted.



Evidence for Galaxy Formation Processes

The fact that galaxies of different morphologies prefer different environments clearly tells us something about how these galaxies form. There are two main hypotheses:

1. in the **monolithic collapse** picture, galaxies of different morphologies preferentially formed in different environments and have remained there since; whereas
2. in the **hierarchical growth** picture the initial building blocks for galaxies formed in all environments, but those in regions of high galaxy density tended to undergo more interactions, which shaped their eventual appearance.

It is difficult to see how the first scenario could have occurred naturally, whilst the second hypothesis is much easier to imagine.

There is now a wealth of **observational evidence** to support the hierarchical picture. Here we give just a few examples.

- **cD galaxies** in the cores of rich clusters are almost definitely the products of multiple galaxy mergers. Numerical simulations support this interpretation and can reproduce the extended light profiles observed in cD galaxies (see Figure 4.7). *Refer back to Section 1 for an introduction to surface brightness profiles.*
- X-ray observations also show evidence for ongoing **cannibalism** of cluster galaxies by the central cD galaxy. An example of cannibalism in the core of a cluster is shown in Figure 4.8 for the Perseus cluster. Here, the presence of X-ray voids indicates that the gas is not completely relaxed. Since cD galaxies are very similar to ellipticals, apart from the former's more extended envelopes, this suggests that interactions and mergers play an important role in the formation of all early-type galaxies.

Figure 4.7 Schematic surface brightness profile in a cD galaxy (dashed line) compared to an elliptical (solid line). The radius encircling half the light in a galaxy is called the effective radius r_e .

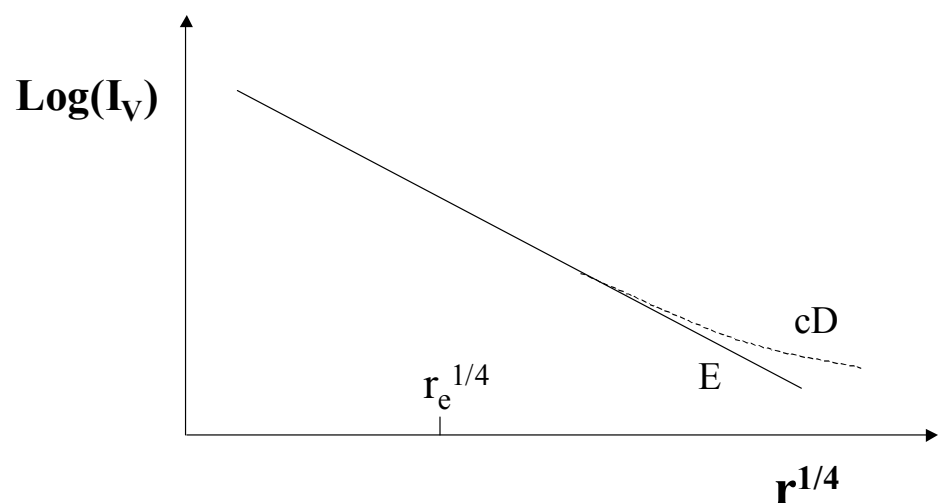
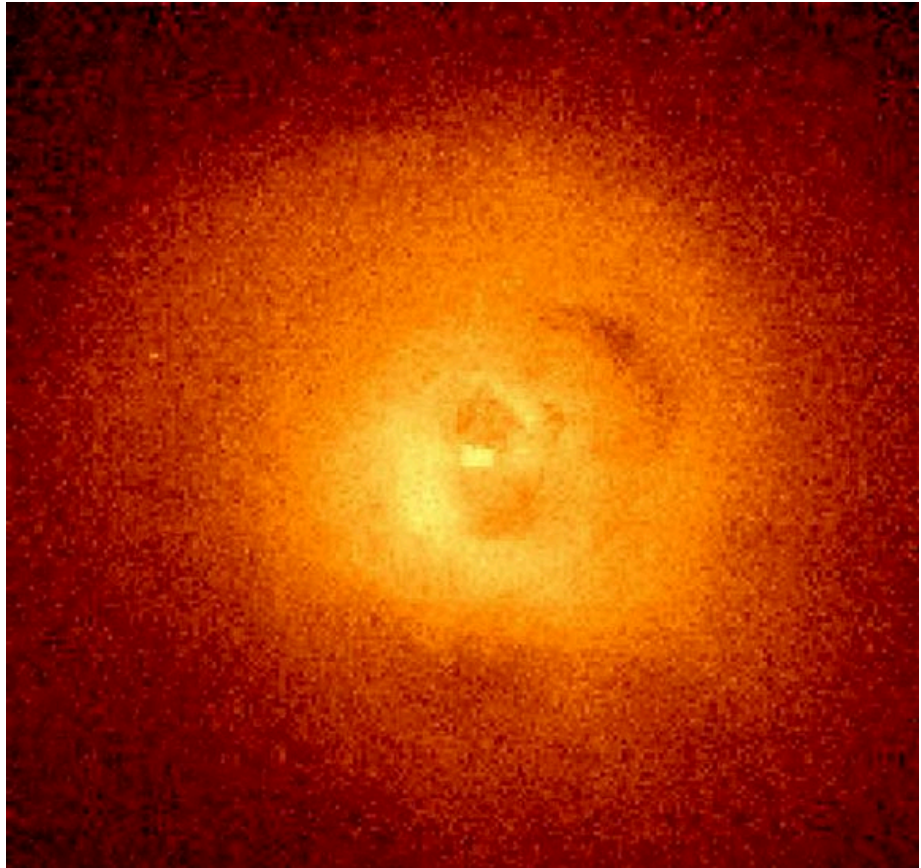


Figure 4.8 X-ray image of the Perseus cluster taken with the Chandra satellite. Image scale is 6.5 arcmins square, centred on RA=03h19m48.1s, Dec=+41°30'42", (equinox 2000).
Image credit:
NASA/IOA/ A. Fabian et al.

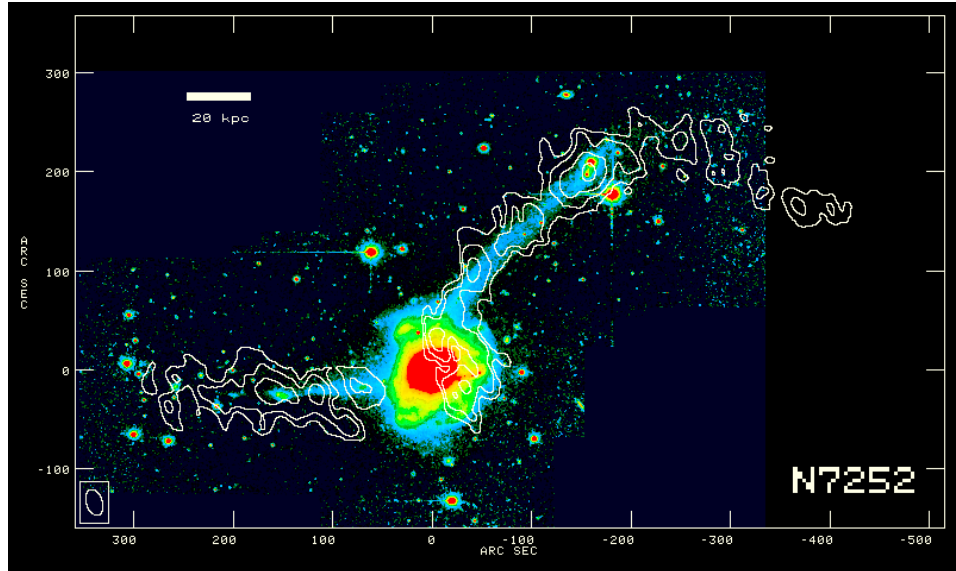


- **Interactions** of galaxies are common, as we saw from the examples in the Local Group (Section 3 of these *Notes*). **Mergers** of similar-mass galaxies lead to more catastrophic changes in morphology. Again, numerical simulations support the hypothesis that a merging pair of gas-rich spirals forms a single elliptical galaxy, once the pair has coalesced under gravity.
- Observational evidence of this merger process is seen in the local universe, in galaxies such as NGC 7252 (Figure 4.9). In terms of its surface brightness profile, colours and kinematics, this galaxy is elliptical-like in its central regions. In its outer regions, it has two **tidal tails** consisting of stars and cold gas. This indicates that there were originally two cold, gaseous discs. If the original galaxies had been ellipticals then their high velocity dispersions would have prevented any narrow, kinematically cold, tidal structures from forming when the galaxies merged. In general, morphologically narrow features such as tails and bridges must originate from progenitor galaxies with strong streaming motions such as the rotational motions in disc galaxies but relatively low velocity dispersions.
- In the **monolithic collapse** hypothesis, the stars in ellipticals were rapidly made from primordial gas together with some later **self-enrichment**, until star formation stopped early on in the life of the universe. Therefore we would expect the stars in ellipticals to be uniformly old, and to be generally metal-poor. However, spectroscopic studies reveal that this is not the case. Stellar populations in elliptical galaxies are generally metal-rich and show a

S
E
I
X
I
G
A
G

range of luminosity-weighted average ages. This is particularly true for ellipticals outside rich clusters. These properties are, on the contrary, a natural part of the hierarchical picture.

Figure 4.9 NGC 7252 – an elliptical galaxy in the making. This false colour image shows the optical light from the merger remnant. Overlying contours show the distribution of neutral hydrogen gas, extending out beyond the optical tidal tails.
Image credit: J. Hibbard, NRAO



- Evidence for high metallicity in elliptical galaxies comes from the strength of heavy-element absorption lines in their spectra. See for example *S&G*, Figure 6.17 and compare this spectrum with the stellar spectra shown in Figure 1.5, Section 1 of these *Notes*, and note the similarity with stars of spectral type K. This is due to the fact that red giant (especially KIII) stars dominate the light of elliptical galaxies.

Exercise 3



Imagine you could observe galaxies with arbitrarily high spatial resolution. In such an ideal case, suggest observations you could carry out which would support or refute one or other of the two broad formation processes (monolithic versus hierarchical).

Exercise 4



Obtain a Digital Sky Survey image from the web of the same region of the Perseus cluster as shown in Figure 4.8. Notice the highly extended distribution of optical light in the central cD galaxy Perseus A, compared with other elliptical galaxies in this cluster.

light (i.e. very little information). This is known as the **cosmic dark ages**. Light from galaxies and quasars is observed from the end of this dark age, until the current time.

When Did Galaxies First Appear?

End of the Dark Age

The most distant galaxies and quasars are observed after the end of the dark age, once star formation had begun in earnest. At that time black hole formation in the cores of forming galaxy spheroids was also occurring. So non-stellar emission also contributes to light seen after the dark age, in the form of active galactic nuclei in quasars. Gamma-ray bursts (GRBs) may also be visible out to quite large redshifts. Let us have a look at how far back we can see these different objects.

One of the most distant **quasars** known was detected in the **Sloan Digital Sky Survey** (SDSS) in the US, in which low resolution optical spectra have been obtained for many sources in particular areas of sky. The source **SDSSJ1148+5251** is at $z = 6.43$. Large quantities of dust have been found in this quasar (see <http://www.ras.org.uk/> press releases), implying the presence of heavy elements. This result was announced on *2 April 2003*.

One of the most distant **galaxies** known was confirmed from optical spectroscopic observations with the Japanese 8 metre **Subaru** telescope in Hawaii. A candidate was confirmed as a very distant galaxy at $z = 6.58$ (see <http://news.bbc.co.uk/2/hi/science/nature/2884411.stm>). This result was announced on *25 March 2003*. It was detected using a narrow band filter imaging survey to weed out likely candidates, followed by optical spectroscopy to determine the redshift from the **Lyman alpha emission line**. The Lyman line emission comes from star formation in galaxies.

Exercise 4

Search the web for discoveries of distant galaxies, quasars and GRBs. Note down any that supersede the above cases and report these in the discussions on WebCT. What are their redshifts and how were they discovered (what instruments and techniques were used)?

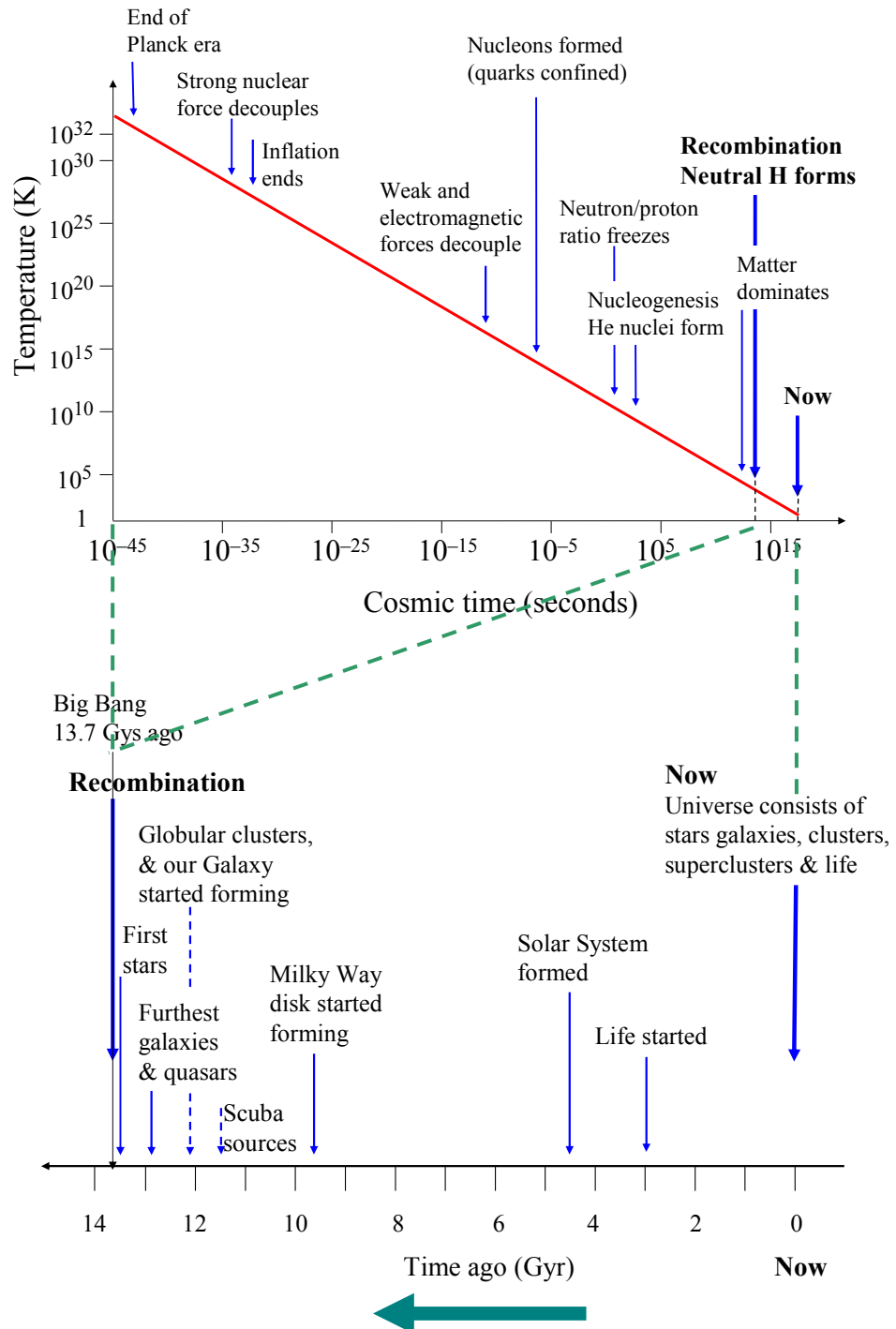
Notice that the most distant galaxies and quasars are seen out to about the same redshift. This redshift ($z \sim 6.5$) corresponds to $\sim 9 \times 10^8$ years after the big bang, assuming the cosmological model and parameters determined by the WMAP team. Simulations showing the end of the dark age can be found at http://home.fnal.gov/~gnedin/GALLERY/rei_a.html. This shows how the dark age is expected to end quite suddenly, after the reionization of hydrogen gas by the first stars, and with the formation of galaxies and quasars.

Figure 5.4 below shows the main cosmological events discussed above, plotted against time. The upper part shows events in the early universe, and an expanded version of later times is shown with a linear timescale in the lower part. This lower part shows the ages of events, with uncertain ages shown by dotted arrows. The age when our Galaxy started forming is estimated from the oldest stars in the halo,

SECTION 5 - EVOLUTION

including globular clusters (see *The Milky Way*, Section 4). The onset of formation of the **Galactic disc** is an average age obtained from the i) **radioactive decay** of long-lived isotopes and ii) the luminosity distribution of **cooling white dwarfs** (see the *Certificate in Astronomy*, Section 10; also *Universe*, Section 22.4).

Figure 5.4 Schematic diagram showing the main events in the history of the Universe relevant to galaxy formation and evolution. Top panel: logarithmic time scale. Lower panel: expanded linear timescale.



Galaxies

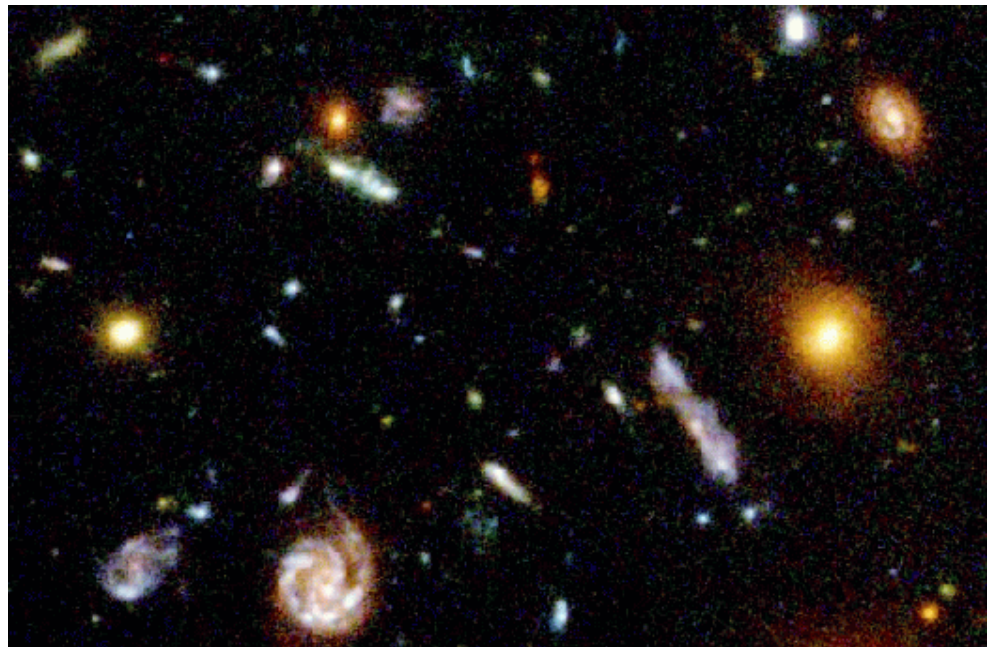
Changes with Look-Back Time

Selection Biases

The distributions of galaxy types and locations in the local universe (described in Sections 1 and 4 of these *Notes*) are not the same when we look back to higher redshifts. Such evolution has been hinted at for a long time (e.g. in apparently changing distributions of galaxy luminosities with redshift). However accurate quantitative comparisons have only become possible from observations made in the last decade or so. This is partly due to the need for appropriately sensitive instruments (e.g. large telescopes, high sensitivity detectors, high spatial resolution) but also due to the many **selection biases** present in observations of samples of distant galaxies. This has resulted in a lack of overlap of distant galaxy samples, making inferences from one sample difficult to test in other wavebands.

It is easiest to detect and measure distances to galaxies with strong **emission lines**. This means galaxies with high levels of star formation or active nuclei. These produce their own spectral signatures and so can be distinguished with spectroscopic or multi-waveband observations. Starburst galaxies show a peaked continuum spectrum, with strong optical emission lines whereas active nuclei emit across a wider range, from radio to X-ray wavelengths. Normal Hubble types with significant emission lines include irregular galaxies and the discs of spiral galaxies, which are forming stars, but not generally E, S0 or other spheroidal types. Therefore, many samples of distant galaxies tend to include a disproportionate amount of star forming or AGN types and undersample the spheroidal stellar populations, where a lot of mass can reside.

Figure 5.5 HST deep field image showing a selection of galaxy morphologies.
Image credit: HDF team, NASA, STScI.



As one goes further out in redshift the light detected in a given filter (say the V band) samples shorter and shorter **rest wavelength** light (see Exercise 1 above). So a visual band survey of nearby versus distant galaxies will not compare like-with-like. The rest frame UV photons sampled from distant galaxies in such a survey will highlight regions of star formation more than the rest frame V band